Monotonic Behavior of High-Strength Steel Unstiffened Extended End-Plate Moment Connections

Fangxin Hu[a,b,*], **Weijie Hou**[a], **Zhan Wang**[a,b]

[a]*School of Civil Engineering and Transportation, South China University of Technology, Guangzhou, 510640, China*
[b]*State Key Laboratory of Subtropical Building and Urban Science, South China University of Technology, Guangzhou, 510640, China*

Abstract

The paper presents experimental investigations on the monotonic inelastic behavior of unstiffened extended end-plate moment connections fabricated from high-strength steel. Three tests were conducted on connections using conventional (grade Q355) steel beams and high-strength (grade Q690) steel columns and end plates. The effect of end plate and column flange thickness was examined, thus resulting in failure modes being either end-plate fracture or bolt rupture. Experimental results are provided in detail, including observations of the two failure modes, moment-drift and moment-rotation curves, and main mechanical indices to characterize inelastic response. The initial rotational stiffness, yield and ultimate moment resistances, and ultimate plastic rotation of these connections, combined with existing experimental results on high-strength (grades Q460, Q690 and Q960) steel end-plate connections, are evaluated and compared with those predicted by Eurocode 3 Part 1-8. The results indicate that the code overestimates the initial stiffness of connections with hand-tightened bolts but underestimates those with preloaded bolts, predicts well the yield resistance, and is acceptable on connection rotation requirements. A more accurate, but simple criterion on connection rotation is proposed.

Keywords: End plate connection, High-strength steel, Moment connection, Monotonic, Joint

[*]Corresponding author
Email address: hufx@scut.edu.cn (**Fangxin Hu**)

1 Introduction

High-strength steels in construction represent a family of steels with a nominal yield stress of 460 MPa (e.g., Q460 in China, or S460 in Europe) and above [1–5]. Their use enables light-weight structures, offering economic and social benefits through reduced material consumption and lower environmental impact, and is also particularly attractive for architectural and aesthetic reasons [6]. To avoid problems of serviceability of structures being dominant, the benefits of the use of high-strength steels can be utilized in braced frames where the stiffness requirement in the form of deflections or drift limits does not govern design. Semi-continuous or partially-restrained connections can be adopted in braced frames to further exploit economic benefits, especially in plastically designed frames [7]. Considering that bolted end-plate connections fall into this category and they are popular due to the simplicity and economy associated to their fabrication and erection, research on high-strength steel end-plate connections is needed to promote their engineering application.

Plastic design of a structure requires the characterization of full nonlinear moment-rotation response of connections, and the connections should be ductile enough to allow for internal force redistribution in the plastic state of the structure. Thus, it is important to design structural connections with enough rotation capacity or ductility [8–11]. The knowledge of the plastic deformation supply of steel members and connections is also very important for steel frames that are expected to experience abnormal loading conditions, such as seismic, fire and impact events, and much concern about the deformation capacity of structural connections has been given by current steel design codes. For example, Eurocode 3 Part 1-8 [12] includes simple deemed-to-satisfy criteria to ensure that the available deformation capacity is greater than the deformation demand of a specific bolted end-plate connection or bolted connection with angle flange cleats. Such simple criteria were mainly derived by Jaspart [13] and Zoetemeijer [14] through thoroughly comparative analysis of the available experimental results of conventional

steel (yield stress lower than 460 MPa) connections. However, as for high-strength steels with higher strength but much higher yield-to-tensile ratio and lower ductility [15–20], the current design criteria are challenged. Since existing studies lack data on the plastic deformation capacity of high-strength steel connections, elastic-plastic structural analysis with these connections acting as plastic hinges is presently not allowed by Eurocode 3 Part 1-12 [21]. To relax these restrictions, several investigations relevant to high-strength steel end-plate connections have been carried out.

Girão Coelho and Bijlaard [22, 23, 24, 25] and Girão Coelho et al. [26, 27] are the first investigators that carried out a number of monotonic loading tests on end-plate connections consisting of conventional steel (S235 and S355) beams and columns, and high-strength steel (S460, S690 and S960) end plates to provide insight into their nonlinear behavior. Test results show that Eurocode 3 Part 1-8 overestimates the rotational stiffness by more than 60% in average, which is in line with previous experimental evidence from connections made up of conventional steels [11], while the code predictions for the plastic resistance compare well with experimental results of the "pseudo-plastic" resistance, which is taken as the intersection between the initial (linear) and post-yield (quasi-linear) phases of a typical moment-rotation curve. The design guidelines for verification of sufficient rotation capacity are conservative in some cases but mostly agree well with the experiments. It was suggested that a minimum supply of plastic rotation, ultimate-plastic resistance ratio, and ductility index, should be taken as 0.035 rad, 1.3, and 4, respectively, to quantitatively lower-bound the rotation capacity requirements in Eurocode 3 Part 1-8. In conclusion, Girão Coelho and Bijlaard [28] proposed amendments to current design provisions in that code, which lead to removing the restrictions of relevant clauses on structural steels up to grades S700. Dubina et al. [29] carried out monotonic and cyclic loading tests on moment-resisting joints of high-strength steel and mild steel components, including twelve bolted stiffened extended end-plate connection specimens. The beams of these connections were all made of mild carbon steel (S235), while the columns of both mild and high-strength steels (S235

and S460) were incorporated. The end plates were realized from three steel grades (S235, S460, and S690) with end-plate thickness determined so as to undergo Mode 2 failure [12]. Test results show that the Eurocode predictions of moment resistance based on the component method agree well with the experimental yield resistances determined following the ECCS procedure [30], and these connections could sustain plastic rotations of 0.05–0.06 rad, to which the contribution of column web panel was as high as 60%–100%, in contrast to the current limit of 30% in the code [12]. So obviously, a larger contribution of web panels than 30% did not adversely affect the rotation capacity of connections. Qiang et al. [31, 32, 33, 34, 35, 36, 37] conducted a series of experimental and numerical studies on the behavior of high-strength steel extended and flush end-plate connections in fire and after fire. As reference, their experimental studies at ambient temperature indicate that, Eurocode 3 Part 1-8 [12] can be applied to high-strength steel extended and flush end-plate connections for predictions of failure mode and plastic flexural resistance, yet the initial rotational stiffness of the tested extended end-plate connections is significantly overestimated. The code provisions on rotation capacity are too conservative, given the fact that all the tested extended and flush end-plate connections not meeting the code-rated ductility requirements sustained maximum rotations of 0.05–0.08 rad and 0.1–0.2 rad, respectively [32, 33]. In contrast to the above-mentioned fire tests under steady-state conditions, Chen et al. [38], Lu et al. [39] and Wang et al. [40, 41, 42] conducted a series of experimental and numerical investigations of high-strength steel extended and flush end-plate connections under transient-state fire conditions, where particularly, creep effect has been incorporated in numerical analysis. Based on the tests at ambient temperature, reasonable agreements between the experimental and predicted plastic resistances using Eurocode 3 Part 1-8 [12] were observed for Q460 steel extended end-plate connections, while the initial rotational stiffness was overestimated [38], which is in accordance with previous findings [32, 43, 44]. But for Q690 steel flush end-plate connections, both the plastic resistance and initial stiffness compare well with predictions [39]. They also found that Q960 steel extended end-plate connections developed

ultimate rotations of 0.07 rad, even much higher than those (0.03–0.07 rad) of Q460 counterparts. The ultimate rotations of Q690 flush end-plate connections were also as high as 0.06–0.1 rad.

The extant investigations demonstrate the great potential of high-strength or even ultra-high-strength end-plate connections to develop sufficient rotation capacity, if the end plate thickness appropriately matches with the bolt grade and diameter to make the end plate in bending predominantly develop plastic deformation [45, 46]. Column web panel (or panel zone) made up of high-strength steel is another joint component with substantial plastic shear distortion capability [47–50], whose interaction with the bolted end plate has not been scrutinized in prior research. It is very likely that the requirements on rotation capacity in Eurocode 3 Part 1-8 [12] are conservative even for high-strength steels. More rational design guidelines are in urgent need. Therefore, in this paper an experimental study was conducted to characterize the stiffness, resistance and rotation capacity of high-strength steel extended end-plate moment connections subjected to monotonic loading. Stiffeners for the extended end plate were not incorporated. The experimental results, combined with prior research findings, were analyzed in a comprehensive way so as to derive practical and reasonable design guidelines on the connections.

2 Test program

2.1 Design of specimens

A reference one-sided end plate connection was designed, representing joints between grade Q355 (conventional-strength) beams and Q690 (high-strength) columns in a 3-bay 6-story prototype plane steel moment frame, as already introduced in previous studies on dual-steel beam-to-column welded flange connections [47]. Such a steel grade combination is rational considering the fact that, the beam design is dominated by deflection requirements under nominal gravity loads in Chinese practice of steel construction, and the application of high-strength steels in beams can hardly bring any benefits. But the design of columns should ensure a strong-column-weak-beam (SCWB) mechanism in addition to strength and stability requirements

under both gravity and seismic load combinations. Thus, using high-strength steels in columns reduces material consumption. In the prototype frame, the beam span (L) is 6 m, while the story height (H) is 3 m. Both beams and columns were made of welded H-sections. The design per Chinese Standard [51] led to beam and column cross-sections of H320×160×8×14 and H200×160×12×16, respectively. Both cross-sections are rather compact, or classified as Class 1 according to Eurocode 3 [52]. It should be noted that the strong-column-weak-beam and panel zone strength were checked according to Eqs. (1) and (2), and the resulting design strength ratios are 1.61 and 1.24, respectively:

$$W_{\mathrm{p,c}} f_{\mathrm{y,c}} \left(1 - \frac{N_{\mathrm{c}}}{f_{\mathrm{y,c}} A_{\mathrm{c}}}\right) \geq \eta_{\mathrm{y}} \Sigma W_{\mathrm{p,b}} f_{\mathrm{y,b}} \tag{1}$$

where $N_{\mathrm{c}}/f_{\mathrm{y,c}}A_{\mathrm{c}}$ is axial load ratio in the column, taken as 0.3 in this study; $W_{\mathrm{p,c}}$ and $W_{\mathrm{p,b}}$ are the plastic section moduli of the column and beam, respectively; $f_{\mathrm{y,c}}$ and $f_{\mathrm{y,b}}$ are the yield strength of column and beam materials, respectively; η_{y} is an overstrength factor taken as 1.1.

$$\frac{4}{3} \frac{f_{\mathrm{y,pz}}}{\sqrt{3}} h_{\mathrm{pz}} b_{\mathrm{pz}} t_{\mathrm{pz}} \geq \alpha_{\mathrm{pz}} \Sigma W_{\mathrm{p,b}} f_{\mathrm{y,b}} \tag{2}$$

where $f_{\mathrm{y,pz}}$ is the yield strength of panel zone materials; t_{pz} is the panel zone thickness, while b_{pz} and h_{pz} represent the width and height of the panel zone, measured as distances between the column flange centerlines and continuity plate centerlines, respectively; α_{pz} is a coefficient taken as 0.95 for one-sided connections.

Bolted end-plate connection in the reference beam-to-column joint was designed according to Chinese Technical Specification [53]. As the design outcome, ten Class 10.9 M20 high-strength bolts were used as shown in Figure 1, meeting the edge distance, bolt spacing, bolt tensile and shear strength requirements. End plates were made of grade Q690 steel in this study, and a minimum end plate thickness was determined as 12.8 mm considering prying action effect. Therefore, the end plate thickness was chosen of 16 mm, which is the same as the column flange

thickness. The resulting connection detail is treated as the benchmark one satisfying all requirements in current Chinese codes. This benchmark connection specimen is labeled as B355-C690-EP16, where the numbers indicate the beam and column steel grades, and the end plate thickness, respectively. To examine the effect of end plate bending strength, another specimen, B355-C690-EP8, was designed by simply using a thinner end plate to replace that in the benchmark specimen (B355-C690-EP16). As the last specimen, labeled as B355-C690-EP16-WCF where "WCF" denotes Weak Column Flange, its column flange was made of 12 mm (i.e., the column H-section is H200×160×12×12), thinner than the benchmark one, thus violating the requirement in Chinese Technical Specification [53] stating that the column flange should be not weaker than the end plate in thickness. This specimen is intended to figure out whether it is probable to further exploit economic benefit by using relatively thin high-strength steel column flanges. Note that this specimen still satisfies the SCWB capacity requirement (the strength ratio indicated by Eq. (1) is 1.31).

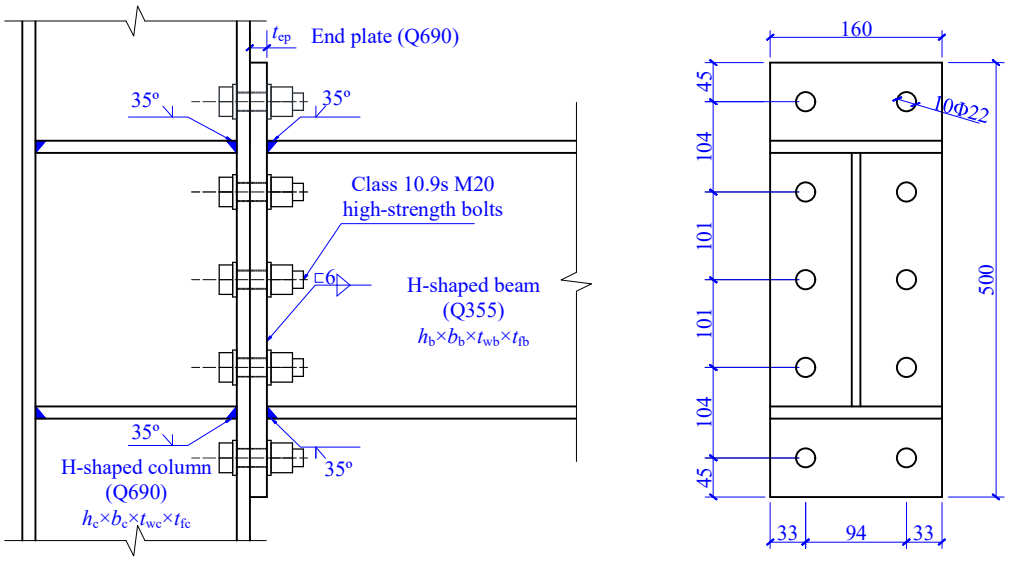

Figure 1. Extended end-plate connection details

As per Chinese Technical Specification [53], complete-joint-penetration (CJP) groove welds were applied between the beam flanges and the end plate, with the beam flange bevels oriented

towards the beam web. A fillet weld was used to reinforce the weld root, while a double-sided fillet weld between the beam web and the end plate ensures adequate shear capacity. It was confirmed that a fillet weld with a 6 mm leg size suffices for shear transfer. Gas-shielded metal arc welding (GMAW) was employed using electrodes matched to grade Q355 steel. Additionally, Chinese Standard [51] prescribes continuity plates in the column web, aligned with the beam flanges and of the same thickness. These continuity plates were connected to the column flanges via CJP groove welds, and to the column web via double-sided fillet welds of 6 mm.

2.2 Material properties

The measured properties of grade Q355 and Q690 steel plates used in this experimental study are summarized in Table 1, including the modulus of elasticity (E), the yield or proof strength (f_y), the strain at the end of the yield plateau (or at the initiation of strain hardening, ϵ_{st}) if applicable, the ultimate strength (f_u), the strain at the ultimate strength (ϵ_u), the yield-to-tensile strength ratio (f_y/f_u), and the percentage elongation after fracture based on a specified parallel length of 50 mm (δ). It should be mentioned that, two 12 mm-thick steel plates of different batches were used. The column web of Specimen B355-C690-EP16 was fabricated from one plate (I), while the column web of Specimen B355-C690-EP8 used the the other plate (II), so did the column in Specimen B355-C690-EP16-WCF. The full-range engineering stress-strain curves of these Q690 steel coupons can be found in previous studies by the authors [47, 48].

Simple tensile testing was also conducted on the class 10.9s M20 high-strength bolt employed in this study. Its modulus of elasticity (E), ultimate strength (f_u), and strain corresponding to the ultimate strength (ϵ_u) are included in Table 1.

2.3 Test setup and loading

The test setup, depicted in Figure 2, involves a beam-to-column connection specimen secured within a large-scale reaction frame. Unidirectional hinge supports were positioned at both column ends to simulate the column's inflection points in the prototype frame, approximately half the

Table 1. Material properties

Steel grade	Plate thickness (mm)	E (GPa)	f_y (MPa)	ϵ_{st}	f_u (MPa)	ϵ_u	f_y/f_u	δ
Q355	8	205.0	406	0.014	539	0.153	0.75	25%
	14	203.5	368	0.020	522	0.200	0.70	29%
Q690	8	208.3	723	—	822	0.100	0.88	20%
	10	189.4	794	—	902	0.106	0.88	21%
	12(I)	205.8	775	0.018	816	0.060	0.95	16%
	12(II)	203.7	660	—	749	0.079	0.88	17%
	16	219.8	811	0.022	840	0.055	0.97	17%
10.9s	M20	206.0	—	—	1135	0.110	—	—

story height. Consequently, the distance between the upper and lower hinge supports represents the story height, or 3000 mm. The column top hinge support was connected to a jack, capable of a maximum load of 300 t, to apply a compression of 30% the axial squash load on the column. An actuator, with a maximum load of 30 t and a stroke of ±250 mm, was attached to the beam end to apply vertical monotonic load. The loading point at the beam end simulates the beam's inflection point in the prototype frame, with the distance from the column centerline to the loading point representing half-span distance of 3000 mm. A lateral restraint system was installed near the beam-end loading point to prevent lateral instability. A roller contact between this device and the beam was installed to minimize friction.

The loading protocol comprises two stages. At the preloading stage, all instruments were checked and reset to zero values initially; a vertical force equal to 20% of the estimated yield load was applied at the beam end, followed by complete unloading, and all readings were verified to return to zero upon unloading. At the formal loading stage, displacement-controlled loading was applied incrementally until specimen failure occurred (e.g., specimen fracture, bolt rupture, or a sudden drop in load without further increase), at which point the test was terminated immediately.

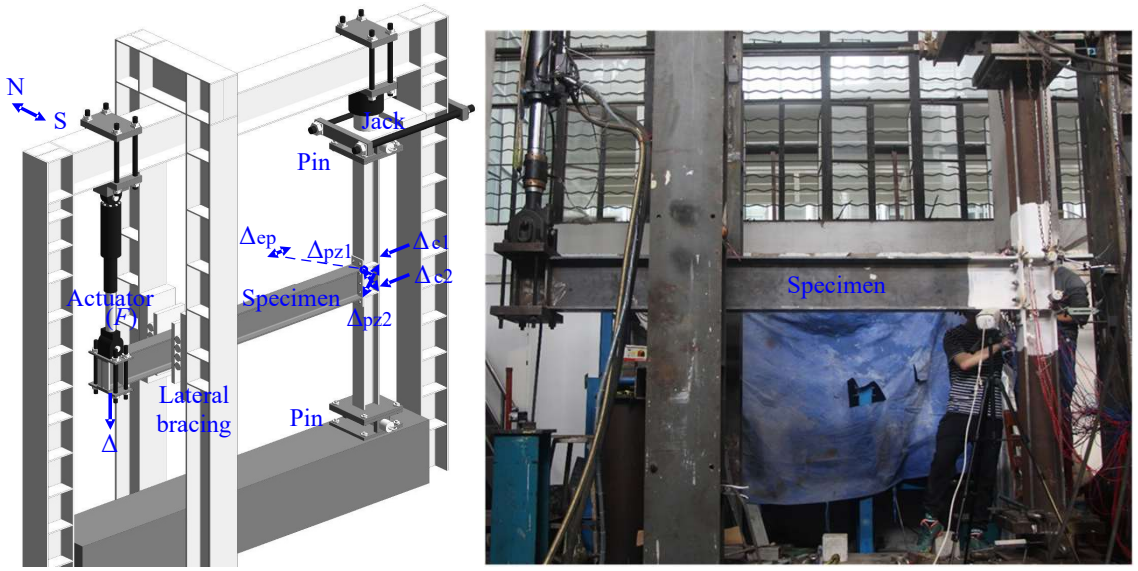

(a) Scheme (b) On site

Figure 2. Test setup

2.4 Instrumentation

As shown in Figure 2(a), the actuator force, F, was measured by the actuator's built-in load cell, with push force defined as positive and pull force as negative. The measured displacements include: beam-end displacement (Δ), obtained using a wire potentiometer; diagonal distance variations (Δ_{pz1} and Δ_{pz2}) at the joint panel zone corners, measured via wire potentiometers; horizontal displacements (Δ_{c1} and Δ_{c2}) at the column flanges aligned with the centerlines of the upper and lower continuity plates, recorded using Linear Variable Differential Transformers (LVDTs); horizontal gap opening (Δ_{ep}) at the end-plate location aligned with the centerline of the beam top flange, also measured via a LVDT. All displacements follow the positive direction indicated by the arrows in Figure 2(a).

The story drift angle (SDA), φ, which is usually used for seismic performance evaluation of steel moment frames, is indicative of the inelastic performance of the whole beam-to-column subassembly. It is defined as:

$$\varphi = \frac{\Delta}{L/2} \tag{3}$$

The SDA consists of deformations of the beam, the column, and the rotation of the end-plate connection (θ) including the shear distortion (γ) of the panel zone and the opening gap rotation (ϕ) between the end plate and column flange:

$$\gamma = \frac{\Delta_{pz1} - \Delta_{pz2}}{2} \frac{\sqrt{b_{pz}^2 + h_{pz}^2}}{b_{pz} h_{pz}} \tag{4}$$

$$\phi = \frac{\Delta_{ep}}{h_b - t_{fb}} \tag{5}$$

where b_{pz} and h_{pz} represent the width and height of the panel zone, measured as distances between the column flange centerlines and continuity plate centerlines, respectively; h_b denotes the beam depth.

3 Test results

3.1 Failure modes

Specimen B355-C690-EP16 failed by bolt fracture, as shown in Figure 3. The outer bolts (first row, outside the beam tension flange) in the extended end plate suddenly fractured when the beam tip displacement reached 175 mm, while the inner bolts (second row, just inside the beam tension flange) exhibited significant necking, though not fractured yet. The extended end plate on the tension side developed moderate plastic deformation, with the lower portion below the middle bolt row remaining in full contact with the column flange. No micro-cracks were observed in the end plate during testing.

Specimen B355-C690-EP8 failed through end-plate fracture, as illustrated in Figure 4. When the beam tip displacement reached 190 mm, cracking initiated in the tension-side extended end plate and propagated rapidly, resulting in complete cross-sectional fracture. All bolts remained essentially undeformed, and the end plate maintained full contact with the column flange both above the first bolt row and below the second bolt row.

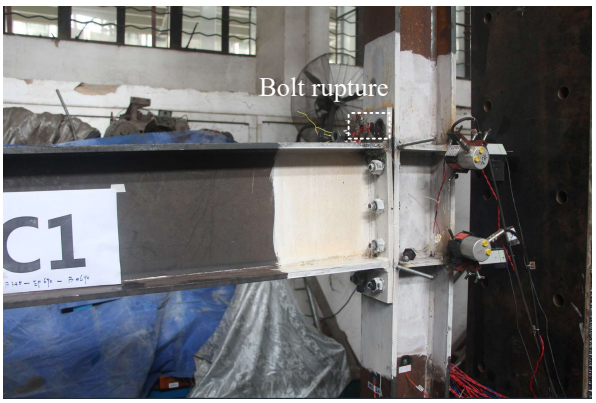

Figure 3. Failure mode of Specimen B355-C690-EP16

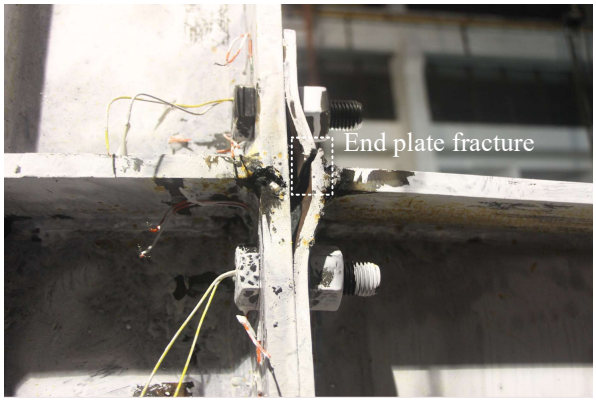

Figure 4. Failure mode of Specimen B355-C690-EP8

For Specimen B355-C690-EP16-WCF, when the beam tip displacement attained 210 mm, the welded steel plates on both sides of the beam extended beyond the lateral restraining device, inducing torsional deformation in the beam and preventing further load increase, as shown in Figure 5. Notably, the joint itself did not experience ultimate failure in this specimen.

3.2 Moment–SDA curves

The moment–SDA (M-φ) relationships of all specimens are presented in Figure 6, where M corresponds to that at the column face, $M_{p,b}$ and $M_{y,b}$ denote the actual full-section plastic moment and flange yield moment of the beam, respectively, computed using the measured steel properties.

As observed from Figure 6, for Specimens B355-C690-EP16 and B355-C690-EP16-WCF, the beam sections began to yield when the SDA reached 2.9% and 3.6%, respectively. Plastic hinges

Figure 5. Failure mode of Specimen B355-C690-EP16-WCF

formed at the beams when the SDA attained 4.6% and 6.1%, respectively. These observations demonstrate that both the connections and beams in these specimens exhibited inelastic behavior.

In contrast, Specimen B355-C690-EP8 maintained its maximum column-face moment below the beam's yield moment $M_{y,b}$ throughout the test, indicating that the beam remained elastic while all nonlinear response originated from the connection behavior.

3.3 Moment–rotation curves

Moment–rotation curves are essential to characterize the connection behavior of beam-to-column joints. It has been shown that the beam end close to the end plate developed substantial plastic rotation in some specimens. Therefore, both the shear distortion of the panel zone and the opening gap rotation between the end plate and column flange were monitored continuously in the tests to obtain moment–shear distortion (M–γ) curves for the panel zones of the specimens, and moment-gap rotation (M–ϕ) curves for the end plates, as shown in Figure 7 and 8, respectively.

The total joint rotation (θ) is the sum of panel zone distortion and end plate gap rotation:

$$\theta = \gamma + \phi \tag{6}$$

The moment–joint rotation (M–θ) curves of all specimens are shown in Figure 9.

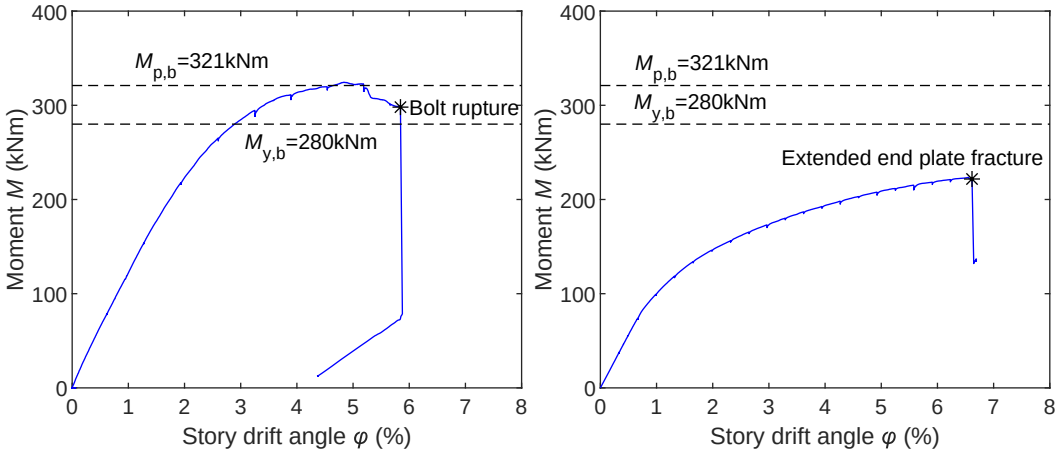

(a) Specimen B355-C690-EP16

(b) Specimen B355-C690-EP8

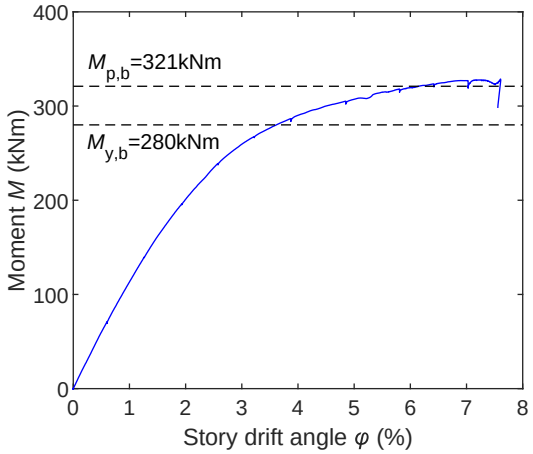

(c) Specimen B355-C690-EP16-WCF

Figure 6. Moment–SDA curves

3.4 Mechanical indices

Based on the moment–joint rotation curves in Figure 9, the elastic stiffness, $S_{j,ini}$, was determined using linear regression on the initial branch. The yield moment resistance, M_y, and the yield rotation, θ_y, were determined using the ECCS approach [30], which is illustrated in Figure 10. The results of these quantities, along with the ultimate moment, M_u, and ultimate joint rotation, θ_u, are set out in Table 2. The end plate gap rotation (ϕ_u) and panel zone distortion (γ_{max}) contributions to the ultimate joint rotation at which bolt or end plate fracture occurred are also listed in this table. Note that Specimen B355-C690-EP16-WCF was not loaded into joint failure;

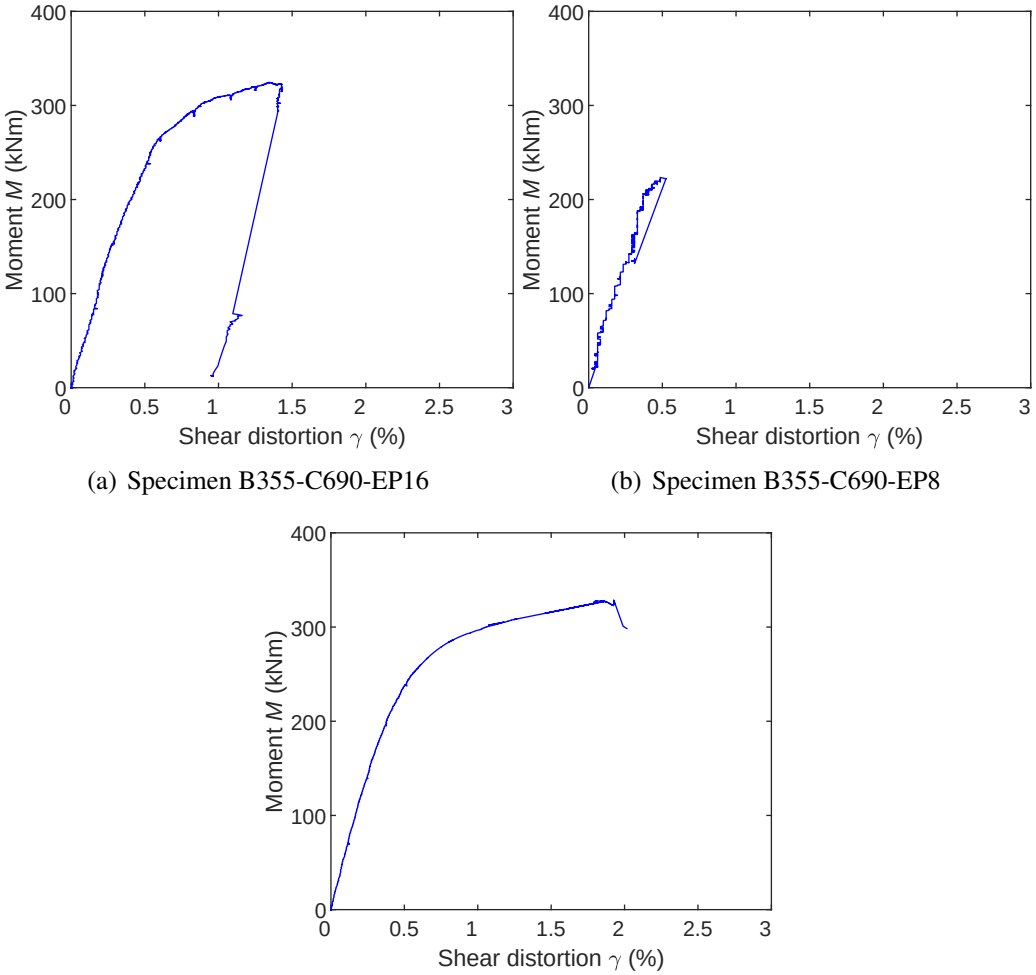

(a) Specimen B355-C690-EP16

(b) Specimen B355-C690-EP8

(c) Specimen B355-C690-EP16-WCF

Figure 7. Moment–shear distortion curves

therefore, the rotation quantities of this specimen in Table 2 are lower bounds on the true rotation capacity of its joint.

Generally, given the same bolt grade and diameter, thicker end plates lead to higher stiffness and moment resistance but smaller rotation capacity, which is evidenced in Table 2. In case of a thinner column flange than the end plate as in Specimen B355-C690-EP16-WCF, the equivalent T-stub on the column flange side becomes dominant over that of the end plate on when evaluating joint plastic resistance according to the component method in Eurocode 3 Part 1-8[12]. Thus, lower yield resistance is observed than the benchmark specimen (B355-C690-EP16), as expected.

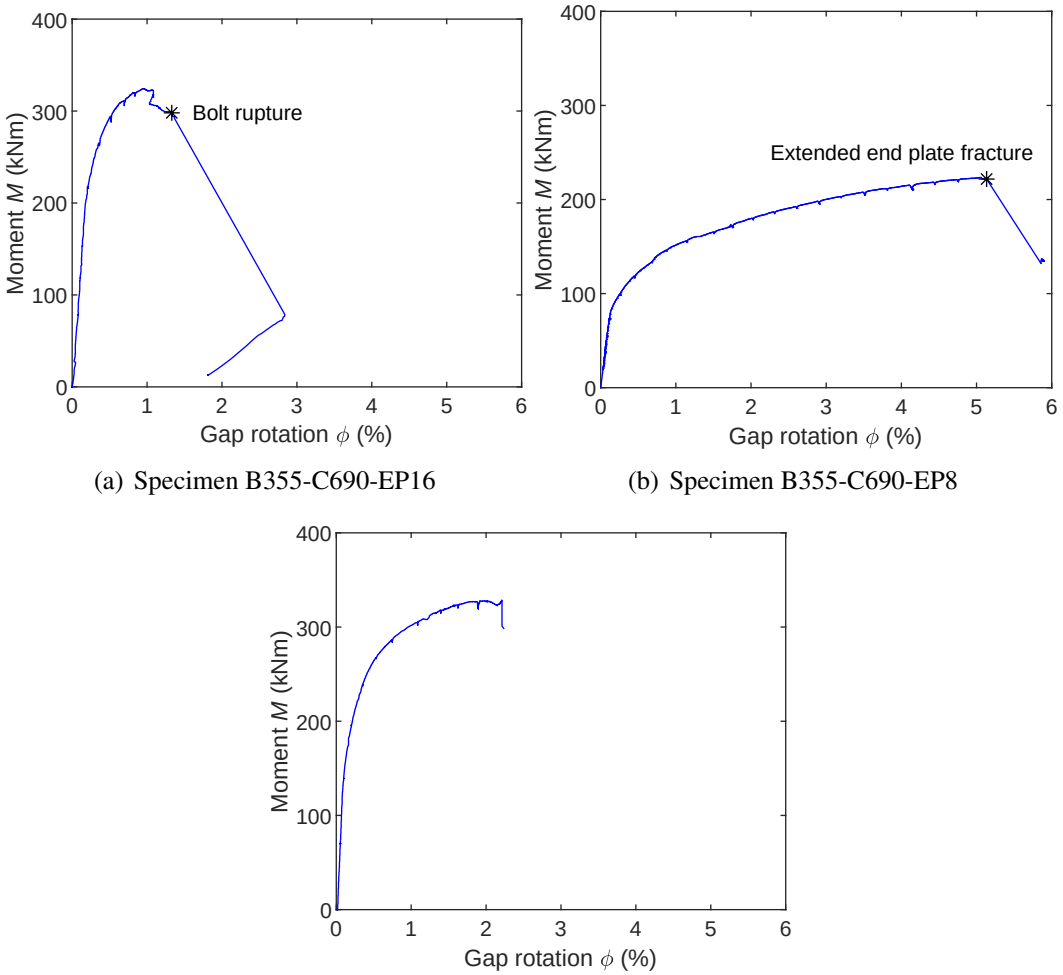

(a) Specimen B355-C690-EP16

(b) Specimen B355-C690-EP8

(c) Specimen B355-C690-EP16-WCF

Figure 8. Moment–gap rotation curves

Interestingly, a thinner column flange also brings a higher gap rotation (or bolted end-plate connection rotation) capacity, based on the comparison between Specimens B355-C690-EP16 and B355-C690-EP16-WCF (note that even Specimen B355-C690-EP16-WCF's ultimate gap rotation should not be limited to 23 mrad shown in Table 2). But the initial rotation stiffness of Specimen B355-C690-EP16-WCF is even higher than Specimen B355-C690-EP16, which is indeed not reasonable, probably due to measurement errors. In addition, the overstrength, described by the ratio, M_u/M_y, is far more significant in the specimen with a thinner end plate (B355-C690-EP8). This is caused by larger strength reserve of the end plate under bending over

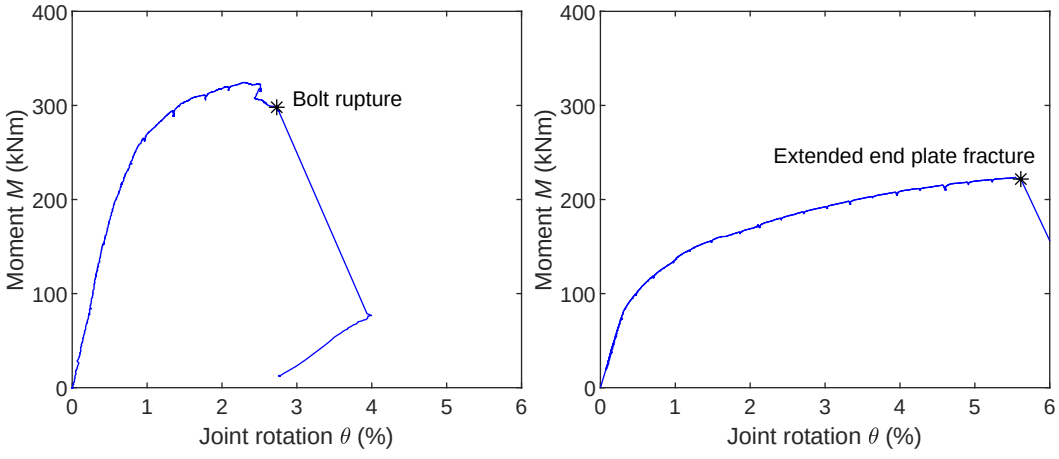

(a) Specimen B355-C690-EP16 (b) Specimen B355-C690-EP8

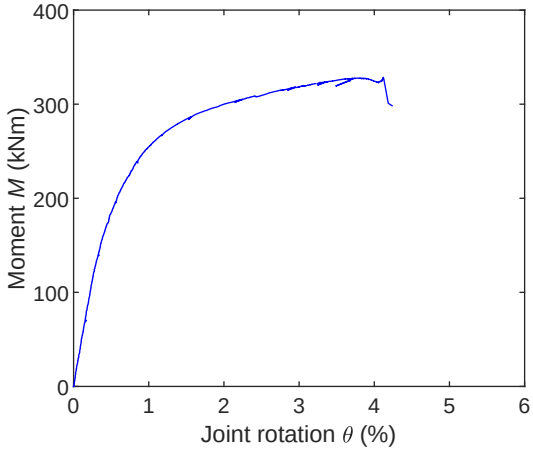

(c) Specimen B355-C690-EP16-WCF

Figure 9. Moment–joint rotation curves

that of the bolt under tension.

4 Discussion

4.1 Design of initial rotational stiffness and moment resistance

To verify whether Eurocode 3 Part 1-8 [12] predictions can apply to high-strength steel joints or not, a comparison between test results and code predictions is undertaken for Q690 high-strength steel joints tested in this paper, as shown in Table 3. The code predictions on joint initial rotational stiffness ($S_{\text{ini,EC3}}$) and plastic resistance ($M_{\text{p,EC3}}$) were evaluated by using the measured material

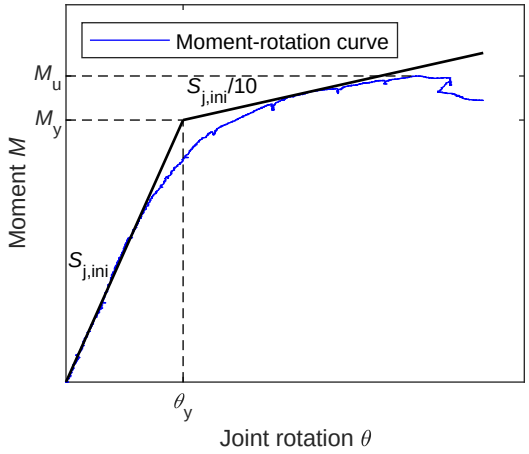

Figure 10. Definition of yield moment and rotation recommended by ECCS [30]

Table 2. Mechanical indices

Specimen label	$S_{j,ini}$ (kNm)	M_y (kNm)	M_u (kNm)	$\frac{M_u}{M_y}$	θ_y (mrad)	θ_u (mrad)	ϕ_u (mrad)	γ_{max} (mrad)
B355-C690-EP16	36235	277.8	324.5	1.17	8	27	13	14
B355-C690-EP8	26649	130.8	223.5	1.71	5	56	51	5
B355-C690-EP16-WCF	44592	241.6	328.7	1.36	5	≥43	≥23	20

properties in Table 1, and the partial safety factors were taken as unitary. Since the quantity of test specimens by the authors is quite limited, previous test results on joints using 460MPa, 690MPa and 960MPa high-strength steel end plates by other investigators [11, 25, 32, 38, 40] were collected as presented in Table 3 as well.

It must be mentioned that the initial rotational stiffness shown in Table 3 does not always correspond to that of the whole joint, which consists of the connection and column web panel. For the three tests in this paper and those conducted by Girão Coelho [11, 25], $S_{ini,EC3}$ does mean the initial rotational stiffness of the joint, as measured moment–joint rotation (M–θ) curves were used to derive experimental stiffness for comparison. Nonetheless, the experimental stiffness reported by Qiang et al. [32], Chen et al. [38] and Wang et al. [40] refers to the bolted end-plate connection only, and the experimental stiffness values were determined via measured moment–connection

Table 3. Predictions by Eurocode 3 Part 1-8 on stiffness and resistance

Specimen label	$S_{\text{ini,exp}}$ (kNm/rad)	$S_{\text{ini,EC3}}$ (kNm/rad)	$\frac{S_{\text{ini,EC3}}}{S_{\text{ini,exp}}}$	$M_{\text{y,exp}}$ (kNm)	$M_{\text{p,EC3}}$ (kNm)	$\frac{M_{\text{p,EC3}}}{M_{\text{y,exp}}}$	$M_{\text{u,exp}}$ (kNm)	$\frac{M_{\text{u,exp}}}{M_{\text{y,exp}}}$
B355-C690-EP16	36235	31206	0.86	277.8	275.5	0.99	324.5	1.17
B355-C690-EP8	26649	17441	0.65	130.8	152.5	1.17	223.5	1.71
B355-C690-EP16-WCF	44592	29935	0.67	241.6	242.8	1.01	328.7	1.36
EEP_15_1[25]	30000	58700	1.96	270	244	0.90	326	1.21
EEP_15_2[25]	35300	58000	1.64	245	369	1.51	366	1.49
EEP_10_2a[25]	17200	31900	1.85	173	184	1.06	244	1.41
EEP_10_2b[25]	19900	34300	1.72	188	184	0.98	252	1.34
EEP_10_3[25]	20700	31900	1.54	235	247	1.05	326	1.39
EEP_10_2(M27)[25]	23200	32800	1.41	195	184	0.94	266	1.36
EEP_10_3(M27)[25]	23000	32800	1.43	253	247	0.98	314	1.24
FS4a[11]	16200	32800	2.02	166	124	0.75	185	1.11
FS4b[11]	17100	32800	1.92	163	124	0.76	188	1.15
JD1[32]	26271	44891	1.71	311.4	279.2	0.90	407.1	1.31
JD2[32]	26297	44891	1.71	317.4	279.2	0.88	395.0	1.24
JD3[32]	17363	31060	1.79	290.5	268.4	0.92	332.4	1.14
J-8-A[38]	23200	26032	1.12	144.2	93.2	0.65	190.7	1.32
J-12-A[38]	28192	46377	1.65	194.9	176.7	0.91	277.7	1.42
JD-A-8[40]	11423	27407	2.40	187.2	190.8	1.02	216.5	1.16
JD-A-12[40]	16231	48666	3.00	320.5	292.0	0.91	365.5	1.14

rotation (i.e., moment–gap rotation, or M–ϕ) curves. As shown in Table 3, Eurocode 3 Part 1-8 [12] underestimates the initial rotational stiffness of the tested joints with preloaded bolts, but overestimates significantly the stiffness obtained in the previous tests. Such a difference may be due to bolt pretension in the tests. In this study, a pretension force of 155 kN per Chinese Technical Specification [53] was applied for class 10.9s M20 high-strength bolts used for the tests, but hand-tightened high-strength bolts were employed by both Girão Coelho [11, 25] and Qiang et al. [32]. The consequence of bolt pretension has been discussed on bolted high-strength steel T-stubs [45], which evidences that Eurcode 3 Part 1-8 [12] does underestimate the stiffness of T-stubs with preloaded bolts. Both Chen et al. [38] and Wang et al. [40] used preloaded high-strength bolts,

but their experimental stiffness values are still much lower than code predictions. There may be experimental measurement errors with their results. Another aspect on the large difference is that, three bolt rows in tension (if the bolt row just above the beam flange in compression is ignored as elaborated in Eurocode 3 Part 1-8 [12]) characterize the specimens in this study, but all specimens in the previous studies [11, 25, 32, 38, 40] feature only two bolt rows in tension, outside or inside the beam tension flange. The comparison in Table 3 shows a possibility that the code leads to stiffness underestimation for more than two bolts rows in tension. This needs further clarification.

As for the design resistance, for most of the test specimens shown in Table 3, the predicted plastic resistance by Eurocode 3 Part 1-8 [12] corresponds well to the experimentally determined yield resistance, except for some large deviations observed in several particular specimens (e.g., Specimens EEP_15_2 [25] and J-8-A [38]). Note that Specimen EEP_15_2 has been particularly recognized as an outlier with meaningless experimental resistance [25]. Therefore, the comparison indicates that Eurocode 3 Part 1-8 [12] can be still applied to joints with high-strength steel end plates of various steel grades, which evidences the conclusions on resistance by Girão Coelho [11, 25].

Values of the experimental ultimate resistance and their overstrength ratios with respect to the yield resistance (i.e., $M_{u,exp}/M_{y,exp}$) are also included in Table 3. The ratios are mostly distributed between 1.15 and 1.7, with an average ratio of 1.3. If the overstrength ratio is evaluated with regard to the code-rated plastic resistance (i.e., $M_{u,exp}/M_{p,EC3}$), the results exhibit a slightly narrower range from 1.2 to 1.5 (note that Specimens EEP_15_2 [25] and J-8-A [38] are excluded as mentioned above), with an average ratio of 1.35.

4.2 Design of ductility requirement

The recommendations on rotation capacity according to Eurocode 3 Part 1-8 [12] are also verified to investigate if they are suitable for high-strength steels, as shown in Table 4. This table summarizes the test results in this paper, as well as the above-mentioned existing experimental results on high-strength steel end-plate joints of various steel grades. In Eurocode 3 Part 1-8 [12],

it is specified that: a bolted end-plate joint may be assumed to have sufficient rotation capacity for global plastic analysis, provided that both of the following criteria are satisfied: (i) the moment resistance of the joint is governed by the resistance of either the column flange or the end plate in bending, and (ii) the thickness, t, of either the column flange (t_{fc}) or end plate (t_{ep}) – not necessarily the same component as (i) – fulfills:

$$t \leq t_{\mathrm{EC3}} = 0.36 d_{\mathrm{b}} \sqrt{\frac{f_{\mathrm{u,b}}}{f_{\mathrm{y}}}} \tag{7}$$

where $f_{\mathrm{u,b}}$ and d_{b} are the tensile strength and diameter of the bolt, respectively; f_{y} is the yield strength of the relevant component (i.e., the column flange, or end plate). The results based on measured properties are set out in Table 4 as well as the ratio t_{EC3}/t, whose values not less than 1.0 indicate compliance with the code requirement. Note that for almost all the specimens, the relevant component is the end plate. The only exception is Specimen B355-C690-EP16-WCF, where the column flange is "weaker" than the end plate (or say, the ratio, t_{EC3}/t, is larger for the column flange compared with the end plate), and so f_{y} and t represent properties of the column flange for this specimen.

No quantitative rules are given in Eurocode 3 Part 1-8 [12] as to how much rotation capacity can be deemed as sufficient. Wilkinson et al. [54] suggest that a moment connection in steel moment resisting frames in a seismic area must develop a minimum plastic rotation of 30 mrad. Girão Coelho and Bijlaard [25] suggest a lower bound requirement of 35 mrad for sufficient ductility. To validate such requirements, the experimental values of connection plastic rotation, $\phi_{\mathrm{u,p}}$, were computed as shown in Table 4. To ensure consistent comparison and assessment, the connection plastic rotation is defined, as employed by Girão Coelho and Bijlaard [25], as the

Table 4. Predictions by Eurocode 3 Part 1-8 on rotation capacity

Specimen label	f_y (MPa)	t (mm)	$f_{u,b}$ (MPa)	d_b (mm)	t_{EC3} (mm)	$\frac{t_{EC3}}{t}$	β	β_{12}	$\phi_{u,p}$ (mrad)
B355-C690-EP16	811	16	1135	20	8.5	0.53	0.83	0.53	12
B355-C690-EP8	723	8	1135	20	9.0	1.13	0.18	0.53	49
B355-C690-EP16-WCF	660	12	1135	20	9.4	0.79	0.83	0.53	≥21
EEP_15_1[25]	483	15	940	24	12.1	0.79	0.58	0.46	22
EEP_15_2[25]	774	15	1413	24	11.7	0.80	0.57	0.46	15
EEP_10_2a[25]	698	10	1413	24	12.3	1.22	0.24	0.46	38
EEP_10_2b[25]	698	10	940	24	10.0	0.99	0.37	0.46	40
EEP_10_3[25]	952	10	1413	24	10.5	1.05	0.33	0.46	30
EEP_10_2(M27)[25]	698	10	1013	27	11.7	1.16	0.26	0.44	46
EEP_10_3(M27)[25]	952	10	1013	27	10.0	1.00	0.36	0.44	37
FS4a[11]	699	10	917	20	8.2	0.82	0.40	0.44	55
FS4b[11]	699	10	917	20	8.2	0.82	0.40	0.44	58
JD1[32]	763	12	1152	27	11.9	1.00	0.29	0.51	62
JD2[32]	763	12	1152	27	11.9	1.00	0.29	0.51	73
JD3[32]	1000	12	1152	27	10.4	0.87	0.37	0.51	46
J-8-A[38]	481	8	866	27	13.0	1.63	0.13	0.47	27
J-12-A[38]	474	12	866	27	13.1	1.09	0.28	0.47	66
JD-A-8[40]	1022	8	1120	24	9.0	1.13	0.27	0.49	49
JD-A-12[40]	1026	12	1120	24	9.0	0.75	0.62	0.49	55

difference between the ultimate connection rotation, ϕ_u, and the first yielding rotation, ϕ_y, i.e.,

$$\phi_{u,p} = \phi_u - \phi_y \tag{8}$$

$$\phi_y = \frac{2/3 M_{y,exp}}{S_{ini,exp}} \tag{9}$$

where the values of $M_{y,exp}$ and $S_{ini,exp}$ are listed in Table 3.

Although developed from the database of conventional structural steel joints, the code requirement in Eq. (7) ($t_{EC3}/t \geq 1$) is suitable for most of the high-strength steel end plate joint specimens to develop a minimum plastic rotation of 35 mrad, as shown in Table 4. However, this

requirement is still too strict for some specimens. For instance, $t_{EC3}/t = 0.82$ for Specimens FS4a and FS4b [11], and $t_{EC3}/t = 0.87$ for Specimen JD3 [32], but these specimens underwent plastic rotations of 46–58 mrad. Notably, Specimen J-8-A [38] exhibited a low plastic rotation (27 mrad) despite its high t_{EC3}/t ratio of 1.63, even lower than the other counterpart Specimen J-12-A (66 mrad) with same properties other than a thicker end plate. Hence, the plastic rotation of Specimen J-8-A is questionable (note that its experimental yield resistance has been suspicious in Section 4.1). The experimental plastic rotation of Specimen JD-A-12 [40] is questionable as well, as its value is even higher than that of Specimen JD-A-8 with a thinner end plate of the same steel grade. Therefore, these two specimens (J-8-A and JD-A-12) will not be included for verifying the rotation capacity requirement.

The conservatism of Eq. (7) for ductility has been recognized by the authors in the experimental response of Q690 high-strength steel preloaded T-stubs [45], where the limit on thickness is suggested to be 20% higher than that determined by Eq. (7). It is well known that a bolted T-stub may exhibit three failure modes (Modes 1, 2, or 3 in Eurocode 3 Part 1-8 [12]), and it is determined by a dimensionless parameter

$$\beta = \frac{2M_p}{Bm} \tag{10}$$

where $M_p = l_{eff}t^2 f_y/4$ is the plastic moment resistance of the flange of the equivalent T-stub in tension, representing the column flange or end plate in bending, where appropriate, and l_{eff} is its effective length, considering both circular and non-circular patterns; B is the tension resistance of a single bolt; and m is the distance between the bolt axis and the section at the flange-to-web connection where a plastic hinge is expected to form. In fact, Eq. (7) was derived based on the assumption of $\beta \leq 1$ with consideration of material partial safety factors [13]. According to Eurocode 3 Part 1-8 [12], the first bolt row (i.e., the outmost bolt row away from the neutral axis) under tension corresponds to the extended portion of the end plate, which should be the bolt row

demanding the largest deformation to accommodate internal force distributions in joint components given a certain connection rotation. Consequently, the failure mode of the equivalent T-stub modeling the extended portion of the end plate or the corresponding column flange, whichever has lower resistance, determines the expected rotation capacity. Values of β for the equivalent T-stub modeling the first bolt row are set out in Table 4, as well as β_{12} which characterizes the transition between Modes 1 (complete flange yielding, considering the bolt action spread on the area under the washer) and 2 (flange yielding and bolt failure) [45]. The extended portion of the end plate was found to be always the dominant weaker component than the column flange for the specimens in Table 4, even for Specimen B355-C690-EP16-WCF with thinner column flanges than the end plate. This is because of the presence of continuity plates, inducing a much larger effective length of the column flange than that of the end plate.

It is clearly seen from Table 4 that using β instead of t_{EC3} is much better for judging whether the plastic rotation meets 35 mrad or not. A simple criterion is proposed here that sufficient rotation capacity can be anticipated if $\beta \leq \beta_{12}$, which means the failure is dominated by the end plate under bending rather than bolts in tension. Specimens FS4a, FS4b, and JD3, which are recognized as specimens not satisfying Eq. (7), now fall into the qualified group to develop sufficient rotation. The only "outlier" is Specimen EEP_10_3 [25], which is qualified by comparing β but developed $\phi_{\mathrm{u,p}}$ of only 30 mrad. This is not surprising due to the intrinsic high uncertainty regarding ductility or rotation capacity determined by identifying failure.

5 Conclusions

This paper reports on an experimental investigation into the monotonic inelastic response of grade Q690 high-strength steel end-plate beam-to-column connections. A set of three one-sided joint specimens was tested, whose experimental results were combined with other existing experimental results to verify current code provisions on the initial rotation stiffness, resistance and rotation capacity of high-strength steel (grades Q460, Q690, and Q960) end-plate

connections. The study yields the following conclusions:

1) Eurocode 3 Part 1-8 [12] underestimates the initial rotational stiffness by up to 35% for beam-to-column connections with preloaded high-strength bolts and more than two tension bolt rows, while it has been generally recognized that the code overestimates the stiffness for connections with hand-tightened (or snug-tightened) bolts.
2) Eurocode 3 Part 1-8 [12] can be applied to predict the design resistance of high-strength steel end-plate connections. The ultimate resistance is 1.35 times the design plastic resistance on average.
3) Eurocode 3 Part 1-8 [12] is acceptable regarding its rotation capacity requirements to be used for high-strength steel end-plate connections. A more accurate criterion is to use the dimensionless β parameter ($\beta = 2M_p/Bm$) for the equivalent T-stub modeling the first tension bolt row, and setting an upper bound of β_{12}, which characterizes the transition between Modes 1 and 2 failure of the equivalent T-stub, allows for sufficient plastic rotation ($\geq$ 35 mrad).
4) Using thinner column flanges than the end plate contributes to the achievement of higher connection rotation (or gap rotation). Further studies are needed to validate this finding, given the limited sample size.

Acknowledgements

The authors would like to acknowledge the financial supports for this work by the National Natural Science Foundation of China (Grant Nos. 51638009, 52108145, 52478521), Guangdong Basic and Applied Basic Research Foundation (Grant No. 2023A1515010047), Guangzhou Basic and Applied Basic Research Foundation (Grant No. 2024A04J9932), State Key Laboratory of Subtropical Building and Urban Science (Grant No. 2023ZB12) and the Fundamental Research Funds for the Central Universities (Grant No. 2023ZYGXZR098).

References

[1] H.-P. Günther, Use and Application of High-Performance Steels for Steel Structures, International Association for Bridge and Structural Engineering (IABSE), Zürich, Switzerland, 2005.

[2] Y. Fukumoto, New constructional steels and structural stability, Engineering Structures 18 (1996) 786–791. doi:https://doi.org/10.1016/0141-0296(96)00008-9.

[3] R. Bjorhovde, Development and use of high performance steel, Journal of Constructional Steel Research 60 (2004) 393–400. doi:https://doi.org/10.1016/S0143-974X(03)00118-4.

[4] G. Shi, F. Hu, Y. Shi, Recent research advances of high strength steel structures and codification of design specification in China, International Journal of Steel Structures 14 (2014) 873–887. doi:https://doi.org/10.1007/s13296-014-1218-7.

[5] H. Ban, G. Shi, A review of research on high-strength steel structures, Proceedings of the Institution of Civil Engineers - Structures and Buildings 171 (2018) 625–641. doi:https://doi.org/10.1680/jstbu.16.00197.

[6] T. V. Galambos, J. F. Hajjar, C. J. Earls, J. L. Gross, Required properties of high-performance steels, Report No. NISTIR 6004, Building and Fire Research Laboratory, National Institute of Standards and Technology, Gaithersburg, MD, USA, 2000.

[7] C. Faella, V. Piluso, G. Rizzano, Structural Steel Semirigid Connections: Theory, Design and Software, CRC Press, Boca Raton, Florida, USA, 2000.

[8] D. Beg, E. Zupančič, I. Vayas, On the rotation capacity of moment connections, Journal of Constructional Steel Research 60 (2004) 601–620. doi:https://doi.org/10.1016/S0143-974X(03)00132-9.

[9] R. Bjorhovde, Deformation considerations for connection performance and design, in: F. S. K. Bijlaard, A. M. Gresnigt, G. J. van der Vegte (Eds.), Proceedings of the Fifth International Workshop on Connections in Steel Structures: Behavior, Strength & Design, Bouwen met Staal, Amsterdam, The Netherlands, 2004, pp. 11–20.

[10] V. Gioncu, F. M. Mazzolani, Ductility of Seismic Resistant Steel Structures, Spon Press, London, UK, 2002.

[11] A. M. Girão Coelho, Characterization of the ductility of bolted end plate beam-to-column steel connections, Ph.D. thesis, University of Coimbra, Coimbra, Portugal, 2004.

[12] European Committee for Standardization (CEN), Eurocode 3: Design of steel structures - Part 1-8: Design of joints. EN 1993-1-8:2005, British Standards Institution (BSI), London, UK, 2005.

[13] J.-P. Jaspart, Contributions to recent advances in the field of steel joints: Column bases and further configurations for beam-to-column joints and beam splices, Professorship thesis, University of Liège, Liège, Belgium, 1997.

[14] P. Zoetemeijer, Summary of the research on bolted beam-to-column connections, Report No. 6-90-2, Stevin Laboratory – Steel Structures, Delft University of Technology, Delft, The Netherlands, 1990.

[15] R. Bjorhovde, Performance and design issues for high strength steel in structures, Advances in Structural Engineering 13 (2010) 403–411. doi:https://doi.org/10.1260/1369-4332.13.3.403.

[16] H. Ban, G. Shi, Y. Shi, Y. Wang, Research progress on the mechanical property of high strength structural steels, Advanced Materials Research 250-253 (2011) 640–648. doi:https://doi.org/10.4028/www.scientific.net/AMR.250-253.640.

[17] F. Hu, G. Shi, Constitutive model for full-range cyclic behavior of high strength steels without yield plateau, Construction and Building Materials 162 (2018) 596–607. doi:https://doi.org/10.1016/j.conbuildmat.2017.11.128.

[18] F. Hu, G. Shi, Y. Shi, Constitutive model for full-range elasto-plastic behavior of structural steels with yield plateau: Formulation and implementation, Engineering Structures 171 (2018) 1059–1070. doi:http://dx.doi.org/10.1016/j.engstruct.2016.02.037.

[19] F. Hu, G. Shi, Y. Shi, Constitutive model for full-range elasto-plastic behavior of structural steels with yield plateau: Calibration and validation, Engineering Structures 118 (2016) 210–227. doi:http://dx.doi.org/10.1016/j.engstruct.2016.03.060.

[20] G. Shi, X. Zhu, H. Ban, Material properties and partial factors for resistance of high-strength steels in china, Journal of Constructional Steel Research 121 (2016) 65–79. doi:https://doi.org/10.1016/j.jcsr.2016.01.012.

[21] European Committee for Standardization (CEN), Eurocode 3: Design of steel structures - Part 1-12: Additional rules for the extension of EN 1993 up to steel grades S700. EN 1993-1-12:2007, British Standards Institution (BSI), London, UK, 2007.

[22] A. M. Girão Coelho, F. S. K. Bijlaard, Experimental behaviour of high strength steel end-plate connections, Journal of Constructional Steel Research 63 (2007) 1228–1240. doi:https://doi.org/10.1016/j.jcsr.2006.11.010.

[23] A. M. Girão Coelho, F. S. K. Bijlaard, Ductility of high performance steel moment connections, International Journal of Advanced Steel Construction 3 (2007) 765–783. doi:https://doi.org/10.18057/ijasc.2007.3.4.5.

[24] A. M. Girão Coelho, F. Bijlaard, High strength steel in buildings and civil engineering structures: design of connections, Advances in Structural Engineering 13 (2010) 413–429. doi:https://doi.org/10.1260/1369-4332.13.3.413.

[25] A. M. Girão Coelho, F. S. K. Bijlaard, Behaviour of high strength steel moment joints, Heron 5 (2010) 1–32.

[26] A. M. Girão Coelho, F. S. K. Bijlaard, L. S. da Silva, Experimental assessment of the ductility of extended end plate connections, Engineering Structures 26 (2004) 1185–1206. doi:https://doi.org/10.1016/j.engstruct.2000.09.001.

[27] A. M. Girão Coelho, L. S. da Silva, F. S. K. Bijlaard, Ductility analysis of bolted extended end plate beam-to-column connections in the framework of the component method, Steel and Composite Structures 6 (2006) 33–53. doi:https://doi.org/10.12989/scs.2006.6.1.033.

[28] A. M. Girão Coelho, F. Bijlaard, Moment-resisting joints in high-strength steel: areas for improvement in design standards, Steel Construction 11 (2018) 294–305. doi:https://doi.org/10.1002/stco.201800022.

[29] D. Dubina, A. Stratan, N. Muntean, F. Dinu, Experimental program for evaluation of moment beam-to-column joints of high strength steel components, in: R. Bjorhovde, F. S. K. Bijlaard, L. F. Geschwindner (Eds.), Proceedings of the Sixth International Workshop on Connections in Steel Structures, American Institute of Steel Construction, Chicago, Illinois, USA, 2008, pp. 355–366.

[30] European Convention for Constructional Steelwork (ECCS), Recommended Testing Procedure for Assessing the Behavior of Structural Steel Elements under Cyclic Loads. ECCS TWG 1.3 N. 45, European Convention for Constructional Steelwork, Brussels, Belgium, 2005.

[31] X. Qiang, N. Wu, X. Jiang, Y. Luo, F. Bijlaard, Experimental and numerical analysis on full high strength steel extended endplate connections in fire, International Journal of Steel Structures 18 (2018) 1350–1362. doi:https://doi.org/10.1007/s13296-018-0130-y.

[32] X. Qiang, N. Wu, Y. Luo, X. Jiang, F. Bijlaard, Experimental and theoretical study on high strength steel extended endplate connections after fire, International Journal of Steel Structures 18 (2018) 609–634. doi:https://doi.org/10.1007/s13296-018-0020-3.

[33] X. Qiang, F. S. K. Bijlaard, H. Kolstein, X. Jiang, Behaviour of beam-to-column high strength steel endplate connections under fire conditions – Part 1: Experimental study, Engineering Structures 64 (2014) 23–38. doi:https://doi.org/10.1016/j.engstruct.2014.01.028.

[34] X. Qiang, F. S. K. Bijlaard, H. Kolstein, X. Jiang, Behaviour of beam-to-column high strength steel endplate connections under fire conditions – Part 2: Numerical study, Engineering Structures 64 (2014) 39–51. doi:https://doi.org/10.1016/j.engstruct.2014.01.034.

[35] X. Qiang, X. Jiang, F. S. K. Bijlaard, H. Kolstein, Y. Luo, Post-fire behaviour of high strength steel endplate connections — Part 1: Experimental study, Journal of Constructional Steel Research 108 (2015) 82–93. doi:https://doi.org/10.1016/j.jcsr.2014.10.028.

[36] X. Qiang, X. Jiang, F. S. K. Bijlaard, H. Kolstein, Y. Luo, Post-fire behaviour of high strength steel endplate connections — Part 2: Numerical study, Journal of Constructional Steel Research 108 (2015) 94–102. doi:https://doi.org/10.1016/j.jcsr.2014.10.027.

[37] X. Qiang, Y. Shu, X. Jiang, Y. Xiao, Nonlinear analysis on mechanical behaviour of high strength steel extended endplate connections and equivalent T-stubs in fire considering axial force, Case Studies in Construction Materials 19 (2023) e02402. doi:https://doi.org/10.1016/j.cscm.2023.e02402.

[38] Z. Chen, W. Wang, Z. Wang, Experimental study on high-strength Q460 steel extended end-plate connections at elevated temperatures, Journal of Constructional Steel Research 200 (2023) 107686. doi:https://doi.org/10.1016/j.jcsr.2022.107686.

[39] P. Lu, J. Yang, T. Ran, W. Wang, Experimental study on flexural capacity and fire resistance of high strength Q690 steel flush end-plate connections, Thin-Walled Structures 184 (2023) 110506. doi:https://doi.org/10.1016/j.tws.2022.110506.

[40] W. Wang, Z. Qian, Y. Zhang, Z. Wang, Experimental and numerical study on behaviour of extended end-plate connections with Q960 steel at elevated temperature, Journal of Constructional Steel Research 213 (2024) 108384. doi:https://doi.org/10.1016/j.jcsr.2023.108384.

[41] W. Wang, Z. Chen, L. Zhang, Numerical studies and practical design suggestions on fire resistance of unprotected high-strength steel extended end-plate connections, Fire Technology 59 (2023) 1585–1612. doi:https://doi.org/10.1007/s10694-023-01397-5.

[42] W. Wang, S. Li, T. Ran, Numerical study on high strength Q690 steel flush end-plate connections at elevated temperatures, Fire Technology 60 (2024) 3269–3294. doi:https://doi.org/10.1007/s10694-024-01568-y.

[43] D. Li, B. Uy, J. Wang, Behaviour and design of high-strength steel beam-to-column joints, Steel and Composite Structures 31 (2019) 303–317. doi:https://doi.org/10.12989/scs.2019.31.3.303.

[44] C. Jia, J. Li, Y. Shao, Y. Wang, Parametric analysis of end-plate joint in hybrid strength steel frame subjected to static loads, International Journal of Steel Structures 20 (2020) 1916–1928. doi:https://doi.org/10.1007/s13296-020-00382-w.

[45] T. Lin, Z. Wang, F. Hu, W. Hou, Comparison in tensile behaviour of conventional and high-strength steel welded-plate preloaded T-stubs, Structures 43 (2022) 93–104. doi:https://doi.org/10.1016/j.istruc.2022.06.039.

[46] F. Hu, T. Lin, Z. Wang, Hysteretic energy dissipation capacity of dual-steel welded-plate preloaded bolted T-stubs, Thin-Walled Structures 193 (2023) 111252. doi:https://doi.org/10.1016/j.tws.2023.111252.

[47] F. Hu, Z. Wang, Cyclic behavior of dual-steel beam-to-column welded flange-bolted web connections, Thin-Walled Structures 195 (2024) 111452. doi:https://doi.org/10.1016/j.tws.2023.111452.

[48] F. Hu, Z. Wang, Cyclic behavior of high-strength steel beam-to-column welded flange-bolted web connections, Thin-Walled Structures 201, Part B (2024) 111999. doi:https://doi.org/10.1016/j.tws.2024.111999.

[49] F. Hu, G. Shi, Y. Shi, Experimental study on seismic behavior of high strength steel frames: Global response, Engineering Structures 131 (2017) 163–179. doi:https://doi.org/10.1016/j.engstruct.2016.11.013.

[50] F. Hu, G. Shi, Experimental study on seismic behavior of high strength steel frames: Local response, Engineering Structures 229 (2021) 111620. doi:https://doi.org/10.1016/j.engstruct.2020.111620.

[51] Ministry of Housing and Urban-Rural Development of the People's Republic of China (MOHURD), Standard for design of steel structures. GB 50017-2017, China Building Industry Press, Beijing, China, 2018. (in Chinese).

[52] European Committee for Standardization (CEN), Eurocode 3: Design of steel structures - Part 1-1: General rules and rules for buildings. EN 1993-1-1:2005, British Standards Institution (BSI), London, UK, 2005.

[53] Ministry of Housing and Urban-Rural Development of the People's Republic of China (MOHURD), Technical specification for high strength bolt connections of steel structures. JGJ 82-2011, China Building Industry Press, Beijing, China, 2011. (in Chinese).

[54] S. Wilkinson, G. Hurdman, A. Crowther, A moment resisting connection for earthquake resistant structures, Journal of Constructional Steel Research 62 (2006) 295–302. doi:https://doi.org/10.1016/j.jcsr.2005.07.011.